Available online at www.sciencedirect.com
SCIENCE DIRECT®
Agricultural and Forest Meteorology 129 (2005) 175–185
AGRICULTURAL AND FOREST METEOROLOGY
www.elsevier.com/locate/agrformet

Energy exchange between the atmosphere and a meadow ecosystem on the Qinghai–Tibetan Plateau

Song Gu[a,b,*], Yanhong Tang[a], Xiaoyong Cui[a], Tomomichi Kato[c], Mingyuan Du[d], Yingnian Li[b], Xinquan Zhao[b]

[a]*National Institute for Environmental Studies, Onogawa 16-2, Tsukuba, Ibaraki 305-8506, Japan*
[b]*Northwest Plateau Institute of Biology, Chinese Academy of Sciences, Xining 810001, PR China*
[c]*University of Tsukuba, Tennodai 1-1-1, Tsukuba, Ibaraki 305-8577, Japan*
[d]*National Institute for Agro-Environmental Sciences, Kannondai 3-1-3, Tsukuba, Ibaraki 305-8604, Japan*

Received 2 January 2004; received in revised form 14 December 2004; accepted 23 December 2004

Abstract

To reveal the potential contribution of grassland ecosystems to climate change, we examined the energy exchange over an alpine *Kobresia* meadow on the northeastern Qinghai–Tibetan Plateau. The annual pattern of energy exchange showed a clear distinction between periods of frozen soil with the daily mean soil temperature at 5 cm ($T_{s5} \leq 0$ °C) and non-frozen soil ($T_{s5} > 0$ °C). More than 80% of net radiation was converted to sensible heat (H) during the frozen soil period, but H varied considerably with the change in vegetation during the non-frozen soil period. Three different sub-periods were further distinguished for the later period: (1) the pre-growth period with Bowen ratio (β) > 1 was characterized by a high β of 3.0 in average and the rapid increase of net radiation associated with the increases of H, latent heat (LE) and soil heat; (2) during the growth period when $\beta \leq 1$, the LE was high but H fluxes was low with β changing between 0.3 and 0.4; (3) the post-growth period with average β of 3.6 when H increased again and reached a second maximum around early October. The seasonal pattern suggests that the phenology of the vegetation and the soil water content were the major factors affecting the energy partitioning in the alpine meadow ecosystem.

Keywords: Albedo; Bowen ratio; Eddy covariance; Energy balance; Soil water content

1. Introduction

The Qinghai–Tibetan Plateau with a mean altitude of greater than 4000 m is the highest plateau in the world and it covers about 2.5 million km^2, more than 60% of which is alpine grassland (Zheng, 2000). With its unique topographical and landscape features, the

* Corresponding author. Tel.: +86 971 6141063/81 298 50 2481; fax: +86 971 6141062/81 298 50 2586.
E-mail addresses: gu.song@nies.go.jp, gus@mail.nwipb.ac.cn (S. Gu), tangyh@nies.go.jp (Y. Tang).

0168-1923/$ – see front matter © 2005 Elsevier B.V. All rights reserved.
doi:10.1016/j.agrformet.2004.12.002

plateau has been considered to play an important role in both the physical environments and the ecosystem functions of adjacent regions (Sun and Zheng, 1996; Yabuki et al., 1998a,b; Li et al., 1999). The energy fluxes between the land surface and the atmosphere drive the earth's climate, from local to global scales (Raupach, 1998; Eugster et al., 2000; Kellner, 2001). Recent studies found that the ground temperature of the plateau, particularly in winter, has significantly increased over recent decades (Yao et al., 2000; Liu and Chen, 2000). The changes of climate will affect the energy exchange between an ecosystem and the atmosphere. However, there is a lack of detailed information characterizing the exchange of energy between the atmosphere and the unique alpine ecosystems of the world.

To understand the energy exchange between the plateau ecosystem and the atmosphere, we examined the seasonal variation patterns in the energy flux exchange in a *Kobresia* meadow ecosystem. The alpine meadow represents one of the major grassland ecosystems on the Qinghai–Tibetan Plateau. By focusing on the effects of the high solar radiation, short rainy season, and limited precipitation on the energy exchange, our objectives were limited to (1) characterize the patterns of seasonal and diurnal variation in the energy exchange between the *Kobresia* meadow and the atmosphere and (2) examine the influence of vegetation phenology on the partitioning of energy fluxes.

2. Materials and methods

2.1. Study site

The study site (latitude 37°36′N, longitude 101°18′E, altitude 3250 m) is an alpine meadow dominated by *Kobresia humilis*. The ecosystem is characterized by low temperatures: the annual mean air temperature is −1.7 °C and mean air temperatures in January and July are −15.0 and 10.0 °C, respectively. The annual mean precipitation is 567 mm, of which over 80% falls in the growing season from May to September.

Microclimate conditions during the measurement period were comparable with an average year. The solar radiation (R_s), precipitation, soil water and temperature are presented in Fig. 1. The variation in soil water content was strongly dependent on the precipitation pattern, except during the frozen-soil period when the mean daily soil temperature at 5 cm depth dropped below 0 °C. Monthly mean air temperatures in 2002 showed almost the same seasonal patterns as those for an average year (Fig. 2). The prevailing wind direction is southeast in summer half of the year and northwest in winter half of the year. The soil of the meadow is classified as a Mat-Cryic Cambisol.

Lear area index (LAI) began to increase from late May and reached a maximum of 3.8 in July and then decreased slowly in 2002. The aboveground standing biomass was 282 g m^{-2} on July 30, remained high during August, and then decreased rapidly in September (Kato et al., 2004a,b). Other details are also described elsewhere (Gu et al., 2003).

2.2. Measurements

The eddy covariance method was used to measure the CO_2, sensible heat, and latent heat fluxes at 2.2 m above the ground. We used a CO_2/H_2O infrared analyzer (Li-7500; LI-COR, Inc., Lincoln, NE, USA) and a three-dimensional supersonic anemometer (CSAT-3; Campbell Scientific, Inc., UT, USA) mounted on a horizontal bar extending from a tower. The observation site has a sufficient wide fetch at least 1 km in all directions, but except a 100 m long clay fence of about 1 m high and 250 m long on the east side of the tower. The CO_2/H_2O sensor head was installed in the downwind of the sonic anemometer. The calibration for CO_2/H_2O analyzer was made once half year or so. Short wave and long wave radiation from the sky and the land surface, respectively, were measured with a net-radiometer (CNR-1; Kipp and Zonen) at 1.5 m above the ground. Air temperatures and humidity were measured with a temperature and relative humidity probe (HMP45C; CSI), and wind speeds at 1.1 and 2.2 m above the ground were measured with cup anemometers (034A-L and 014A; Campbell Scientific). Soil water contents were measured with TDR sensors (CS615; CSI) at soil depths of 0.05 m, and soil temperatures were measured with thermocouples from 0.05 m under the ground surface. Soil surface temperatures and soil heat flux (at 0.02 m below the surface) were measured with temperature probes (107; CSI) and

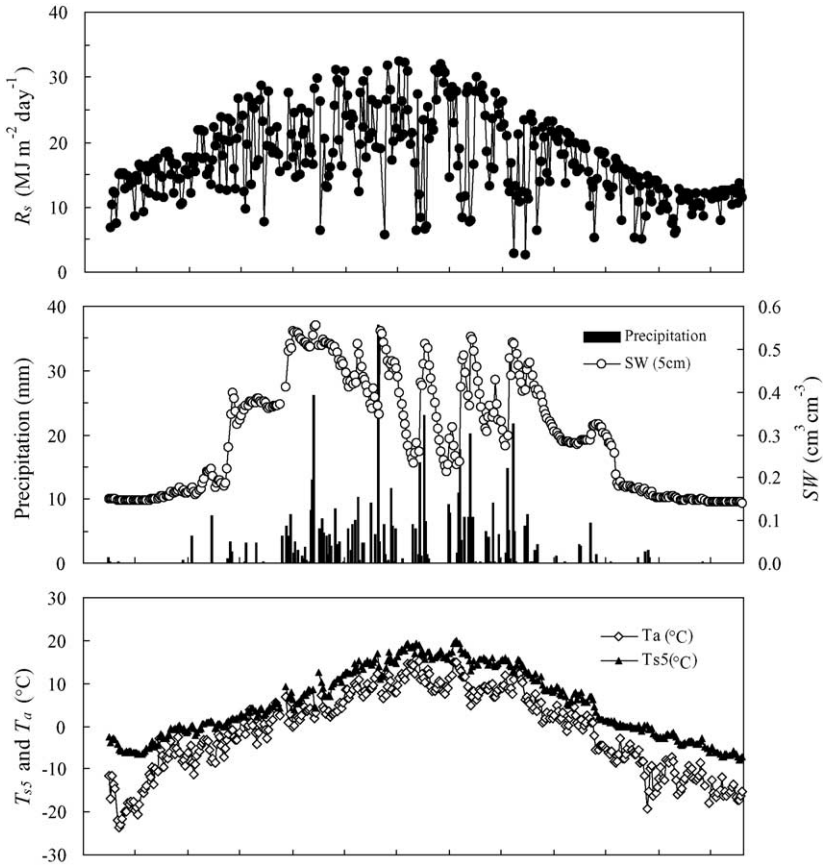

Fig. 1. Seasonal variations of daily-integrated solar radiation (R_s), precipitation, soil water (SW), mean daily air temperature (T_a), and soil temperature at 5 cm depth (T_{s5}) from DOY 15, 2002 to DOY 14, 2003.

heat plates (HFT-3; CSI) buried at three different points at 1 cm below the soil surface; the averaged data was used in our analysis. Precipitation was measured with a tipping bucket rain gauge (TE525MM; CSI) 70 cm above the ground surface. Fluctuations in wind speed, sonic virtual temperature, and CO_2 and H_2O concentrations were sampled by the digital micrologger at 10 Hz. The WPL density correction was then applied to fluxes of CO_2 and water vapor (Webb et al., 1980). The corrections of coordinate rotation, trend removal, and water vapor correlation were made for 10 days in July 2002 by using fluctuation data sampled at the frequency of 10 Hz. The regression line slopes showed very small differences of less than 4% between the corrected and uncorrected fluxes. The bias due to these corrections is likely to be negligible and these correlations were thus not enforced in the current study (see also Kato et al., 2004a,b). Data were recorded with a data-logger (CR23X; CSI) at 15 min intervals. The data from January 2002 to January 2003 are presented in this study.

The net radiation (R_n) is partitioned into sensible (H), latent (LE), and soil (G) heat fluxes:

$$R_n - G = H + \mathrm{LE} + S \quad (1)$$

The storage term (S) can be neglected because it is usually considerably smaller than the other components. The energy balance ratio (r) was calculated using the following equation (Gu et al., 1999):

$$r = \left(\sum(\mathrm{LE} + H)\right) / \left(\sum(R_n - G - S)\right) \quad (2)$$

The item (LE + H) measured by the eddy covariance method seemed underestimated since the average value of EBR was about 0.66 for the entire observation period, which falls in the median region of reported

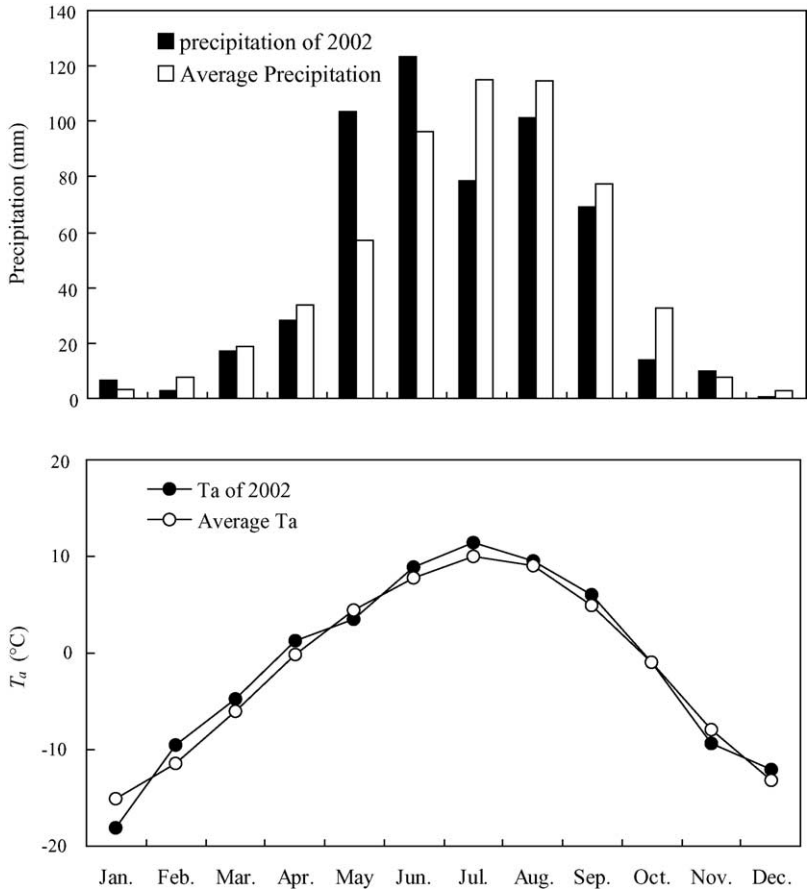

Fig. 2. Monthly precipitation and the average monthly air temperatures (T_a) of 2002, and the averages from 1980 to 2000.

energy closures, which range from 0.55 to 0.99 (Wilson et al., 2002). The lack of energy balance closure has also been reported many times (Stannard et al., 1994; Aubinet et al., 2000), and energy balance closure has become accepted as an important new test of eddy covariance (Anderson et al., 1984; Mahrt, 1998). We were not trying to specify a particular cause for the imbalance because several possibilities may be involved in the lack of energy closure (for details see Wilson et al., 2002).

2.3. Data analysis

Ecosystem surface conductance (g_c) was obtained from the Penman–Monteith equation (Monteith and Unsworth, 1990):

$$1/g_c = \rho C_p d/(\gamma \mathrm{LE}) + (\beta\Delta/\gamma - 1)/g_a \quad (3)$$

where d is the vapor pressure deficit; C_p the specific heat of air at constant pressure; γ the psychrometric constant; ρ the air density; β the Bowen ratio which is H/LE; Δ the slope of the saturation vapor pressure curve at the mean wet-bulb temperature of the air; g_a the air conductance, which can be calculated by Eq. (4) (Monteith and Unsworth, 1990):

$$1/g_a = u/u^{*2} + 6.2u^{*-0.67} \quad (4)$$

where u^* is friction velocity and u is wind speed. Average daily canopy conductance (g_c) was calculated from data collected every 15 min between 11:30 and 15:30 (Beijing Standard Time).We calculated the decoupling coefficient (Ω) according to Jarvis and McNaughton (1986) with Eq. (5):

$$\Omega = (\Delta + \gamma)/(\Delta + \gamma(1 + g_a/g_c)) \quad (5)$$

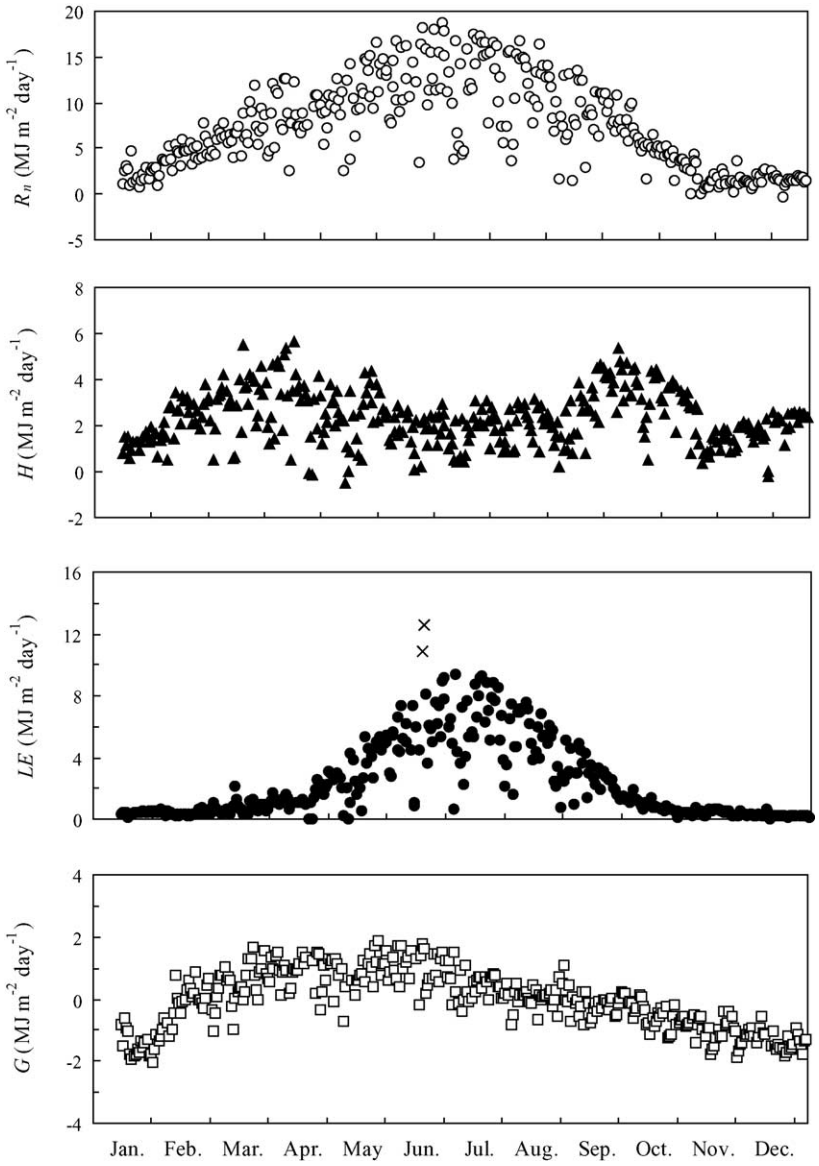

Fig. 3. Seasonal variations of daily-integrated net radiation flux (R_n, ○), sensible heat flux (H, ▲), latent heat flux (LE, ●), and soil heat flux (G, □) from DOY 15, 2002 to DOY 14, 2003. Data marked "×" were considered to be in error and excluded from the analysis.

Data with an event of raining or dewing were not used in the analysis to avoid the possible error caused by liquid water on the sensor window of the CO_2/H_2O analyzer. Data gaps were filled by linear interpolation using the preceding and following data when the gap is in nighttime, daytime gaps were filled by the relationship between solar radiation and measured H or LE.

3. Results and discussion

3.1. Seasonal patterns of energy fluxes and their partitioning

R_n was positive throughout the year-round measurement period (Fig. 3). H increased with the increase of R_n from February, but started to decrease from late

April, even though R_n continued to increase, reaching a minimum in July when the foliage attained its maximum LAI (Fig. 3). H then began to increase again, with a second peak appearing around October. LE started to increase in late April, and the maximum value appeared in late July because the high vegetation coverage and soil water further increased LE during the growth period. When the soil froze in October, the LE became extremely small. G varied between 2.0 and -2.0 MJ m^{-2} day^{-1} and reached a maximum value around June when the vegetation cover was relatively small and solar elevation was high (Fig. 3), and then dropped below zero from early September.

The energy partitioning exhibited distinct seasonal patterns (Fig. 4). The LE/R_n remained almost constant before May and then increased with the developing vegetation foliage, reaching a maximum value in late July with about 0.53 when the LAI was around 3. The lowest value of H/R_n (with around 0.13) appeared during growing period when most of the solar energy received by the ecosystem was consumed in evapotranspiration. From early September, when the grassland foliage showed rapid senescence, there was a rapid increase in H/R_n and a decrease in LE/R_n. The dominant component in the energy balance shifted from LE to H during this period. The ratio of G/R_n appeared to remain relatively steady from the end of February until late October. However, a dramatic change occurred at the beginning of the frozen-soil period from November to February of the following year. This large decline in G/R_n corresponded well with the time that the daily average soil temperature at 5 cm dropped below 0 °C.

The imbalance of energy could change the present results mentioned above. If $(R_n - G)$ is 30% higher than (LE + H), then the values of LE and H will need to increase by a factor of about 30% each if we assume that LE and H increased equivalently in response to some unknown factor, these could result in an underestimation of LE/R_n and H/R_n in the present study.

3.2. Variations in energy flux during different periods

Because of the distinct differences shown in the energy partitioning pattern, we divided the year into two periods: the frozen-soil period (those days when the daily mean soil temperature at 5 cm was equal to or below 0 °C) and the non-frozen-soil period (Table 1). Within the non-frozen period, the seasonal pattern of energy partitioning was mainly dominated by LE and H. We further divided the period into three different sub-periods: the pre-growth period with Bowen ratio (β) < 1, the growth period ($\beta \leq 1$), and the post-growth period ($\beta > 1$). The energy components and the major biometeorological factors were distinct for each of the four periods (Table 1).

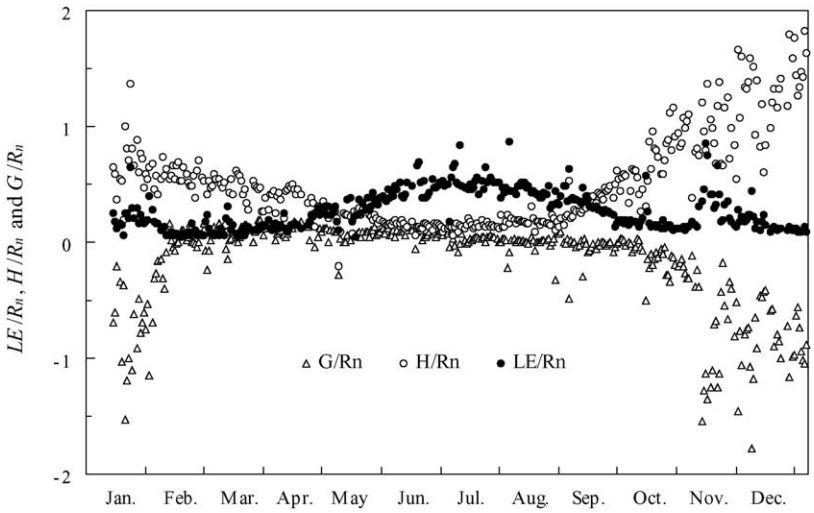

Fig. 4. Seasonal variations of the ratio of energy partitioning (sensible heat flux (H), latent heat flux (LE), and soil heat flux (G)) to net radiation (R_n) from DOY 15, 2002 to DOY 14, 2003.

Table 1
Daily means of solar radiation, energy balance components and major biometeorological factors for each period

	Frozen-soil period (DOY 315–68, 119 days[a])	Non-frozen-soil period		
		Pre-growth period (DOY 69–140, 72 days)	Growth period (DOY 141–263, 123 days)	Post-growth period (DOY 264–314, 51 days)
R_s (MJ m^{-2} day^{-1})	13.0	19.6	21.1	16.9
R_n (MJ m^{-2} day^{-1})	2.7	8.2	11.9	6.5
L_d (MJ m^{-2} day^{-1})	16.5	21.3	26.7	19.9
L_u (MJ m^{-2} day^{-1})	22.9	27.6	31.7	27.0
LE (MJ m^{-2} day^{-1})	0.4	1.3	5.2	1.4
H (MJ m^{-2} day ^{1})	1.9	2.8	2.0	3.5
G (MJ m^{-2} day^{-1})	−0.9	0.7	0.5	−0.4
R_n/R_s	0.21	0.42	0.56	0.38
L_u/L_d	1.39	1.29	1.19	1.36
$(L_u - L_d)/R_s$	0.49	0.32	0.24	0.42
LE/R_n	0.14	0.16	0.44	0.21
H/R_n	0.71	0.34	0.17	0.55
G/R_n	−0.34	0.09	0.04	−0.06
LE/LE$_{eq}$	0.26	0.30	0.66	0.30
Precipitation (mm) (sum)	11.6	121.8	394.7	14.7
T_a (°C)	−12.08	0.06	9.12	−1.38
T_{s5} (°C)	−3.50	3.94	14.79	4.69
SW (m^3 m^{-3})	0.15	0.38	0.40	0.28
Ω	0.19	0.34	0.76	0.27
G_c (mm s^{-1})	2.07	2.17	11.00	2.54
d (kPa)	0.33	0.63	0.75	0.72
α	0.30	0.25	0.20	0.20
β	5.24	2.09	0.39	2.61
LAI	–	–	2.3 (mean)	–

R_s, solar radiation; R_n, net radiation; L_d, long-wave radiation from sky; L_u, long-wave radiation from surface; LE, latent heat flux; LE$_{eq}$, equilibrium evapotranspiration; H, sensible heat flux; T_a, air temperature; T_{s5}, soil temperature at 5 cm depth; SW, soil water at 5 cm depth; Ω, decoupling coefficient; g_c, canopy conductance; d, vapor pressure deficit; α, albedo ratio; β, Bowen ratio; LAI, leaf area index.

[a] Frozen-soil period includes the days from DOY 15 to DOY 68 of 2002 and the days from DOY 315 of 2002 to DOY 14 of 2003.

Most energy flux parameters showed two extremes: one in the frozen-soil period and the other in the growth period (Table 1). All the parameters in the growth period were different from other periods. The patterns of diurnal energy flux variation on clear days differed markedly in different periods of the year (Fig. 5). The clear days were defined as those when transmissivity was greater than 0.7 (Gu et al., 2003). The seasonal change and development of vegetation is one of the major factors determining the diurnal patterns.

During the frozen-soil period, LE was very low with a mean value of 0.4 MJ m^{-2} day^{-1}. Most energy was converted to H, with a mean 1.9 MJ m^{-2} day^{-1}, and G was the minimum, with a mean value of −0.9 MJ m^{-2} day^{-1}. H and G quickly increased with the increase in R_n toward the pre-growth period. However, the most dramatic changes occurred in LE and H during the growth period, when LE rapidly increased and H decreased due to the increases in precipitation and vegetation cover. In this period LE became the dominant component, but H increased again in the post-growth period as LE and G rapidly decreased. The LE at night was near zero throughout the whole measurement period.

3.3. Albedo and Bowen ratio

Daily albedo varied between 0.16 and 0.26 during the non-snow-cover days, but changed little during the growth period from DOY 141 to DOY 263, despite soil water varied between 0.22 and 0.55 m^3 m^{-3}. The higher summertime albedo in comparison with the albedo of lowland ecosystems may favor alpine plants

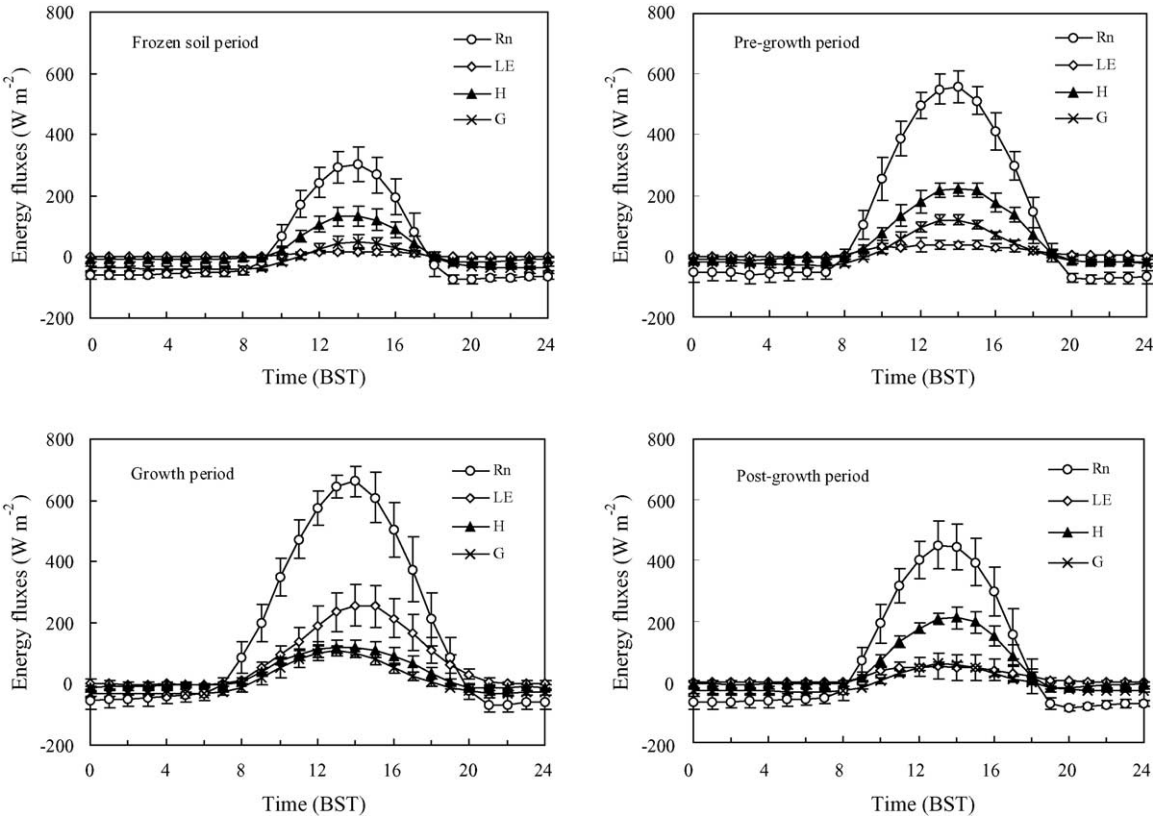

Fig. 5. Averaged diurnal net radiation flux (R_n), latent heat flux (LE), sensible heat flux (H), and soil heat flux (G) for four periods (frozen-soil period from DOY 315 to 68, including the days from DOY 15 to 68, 2002 and the days from DOY 315, 2002 to DOY 14, 2003; pre-growth period from DOY 69 to 140; growth period from DOY 141 to 263; and post-growth period from DOY 264 to 314). Error bars indicate standard error of daily means during the specific period. Only data collected on clear days are presented. Beijing Standard Time (BST) is used here.

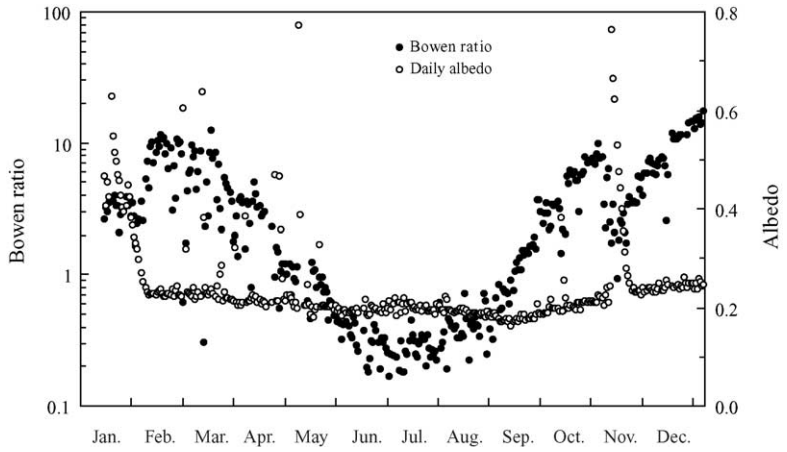

Fig. 6. Seasonal variations in the daily albedo and Bowen ratios from DOY 15, 2002 to DOY 14, 2003.

to avoid the high radiation on the plateau. The lowest albedo occurred in mid-September when foliage began to senesce but while the soil maintained relatively high water content. From then, albedo gradually increased in association with the decreased soil water toward the winter (Fig. 6). The seasonal variation in albedo on the alpine meadow was greatly affected by the vegetation phenology, sky condition, and snow events. Albedo tends to be lower under clear conditions than under cloudy sky conditions. The snow events resulted in high albedo of between 0.3 and 0.8.

β is typically less than 0.2 for tropical oceans and rain forests and larger than 3.8 in arid regions (Eugster et al., 2000). In this study, β ranged between 0.2 and 17 (January 14, 2003) during the measurement period (Fig. 6). The low β in summertime observed in the study may be due to the wet ecosystem. The β increased significantly from early September and peaked in winter. The β decreased markedly when the land surface was covered with snow.

The temporal pattern of g_c in different periods corresponded well with that of LE (Table 1). On clear days, the maximum g_c occurred most often between

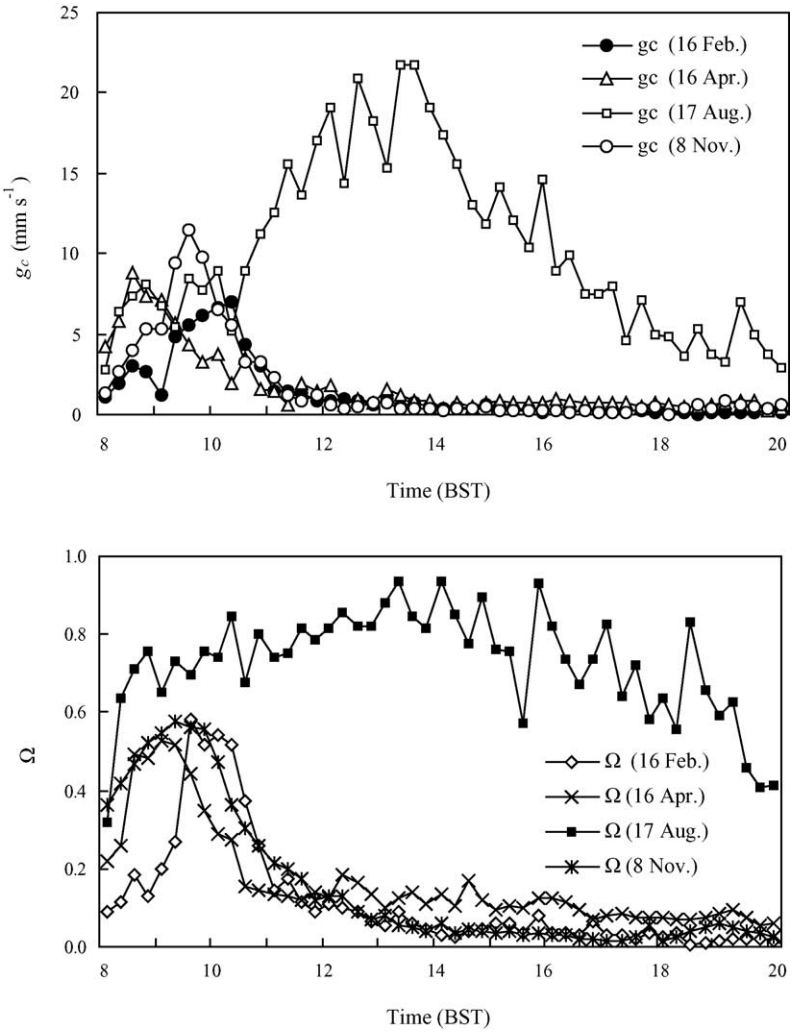

Fig. 7. Diurnal pattern of canopy conductance (g_c) and decoupling coefficient (Ω) on typical clear days in each of the four periods (16 February, frozen soil period; 16 April, pre-growth period; 17 August, growth period; 8 November, post-growth period).

8:00 and 11:00 during the non-growth period. This was mainly due to the surface evaporation from frost or dew limited soil water was evaporated during the midmorning (Fig. 7). During the growth period, the maximum g_c appeared around noon, which indicates sufficient water availability for the ecosystem.

The decoupling coefficient (Ω) provides a tool for separating the effect of d on the LE from that of R_n. To examine the coupling of the ecosystem surface with the atmosphere, we calculated the Ω daily between 11:30 and 15:30 (Table 1). A low Ω indicates a relatively high influence of d on LE, and a high Ω suggests that R_n is the dominant influence on LE (Jarvis and McNaughton, 1986). The high Ω during the growth period indicates that R_n contributed more to the LE than did g_c or d. During the other periods Ω was small, showing that the effect of d was predominant.

The diurnal variation pattern of Ω on typical clear days was similar to the changes in g_c (Fig. 7). This implies that the evapotranspiration of the ecosystem was coupled with d during the pre-growth and post-growth periods, but was coupled mainly with R_n during the growth period.Long-wave radiation is another important factor influencing the energy balance. The magnitude of energy exchanged by long-wave radiation between the surface and the atmosphere exceeds that of short-wave radiation because it is an exchange that continues even at night. In our study, the upward long-wave radiation (L_u) was greater than the downward long-wave radiation (L_d) over the entire measurement period, which indicates that the ecosystem surface lost energy due to the exchange of long-wave radiation. The value of $(L_u - L_d)/R_s$ changed from 0.24 in the growth period to 0.49 in the frozen-soil period (Table 1).

Acknowledgements

This study was supported as a joint research project between the National Institute for Environmental Studies, Japan, and the Northwest Plateau Institute of Biology, Chinese Academy of Science (Grant Nos.: 13575035 and S1 (B13)). The research was also conducted under a Knowledge Innovation Research Project of the Chinese Academy of Science (KZCX1-SW-01-01A).

References

Anderson, D.E., Verma, S.B., Rosenbuerg, N.J., 1984. Eddy correlation measurements of CO_2, latent heat and sensible heat fluxes over a crop surface. Boundary-Layer Meteorol. 29, 263–272.

Aubinet, M., Grelle, A., Ibrom, A., Rannik, Ü., Moncrieff, J., Foken, T., Kowalski, A.S., Martin, P.H., Berbigier, P., Bernhofer, Ch., Clement, R., Elbers, J., Granier, A., Grunwald, T., Morgenstern, K., Pilegaard, K., Rebmann, C., Snijders, W., Valentini, R., Vesala, T., 2000. Estimates of the annual net carbon and water exchange of European forests: the EUROFLUX methodology. Adv. Ecol. Res. 30, 113–175.

Eugster, W., Rouse, W.R., Pielke Sr., R.A., McFadden, J.P., Baldocchi, D.D., Kittel, T.G.F., Chapin III, F.S., Liston, G.E., Vidale, P.L., Vaganov, E., Chambers, S., 2000. Land–atmosphere energy exchange in arctic tundra and boreal forest: available data and feedbacks to climate. Global Change Biol. 6 (Suppl. 1), 84–115.

Gu, J., Smith, E.A., Merritt, J.D., 1999. Testing energy balance closure with GOES-retrieved net radiation and in situ measured eddy correlation fluxes in BOREAS. J. Geophys. Res. 104 (D22), 27881–27893.

Gu, S., Tang, Y., Du, M., Kato, T., Li, Y., Cui, X., Zhao, X., 2003. Short-term variation of CO_2 flux in relation to environmental controls in an alpine meadow on the Qinghai–Tibetan Plateau. J. Geophys. Res. 108 (No. D21), 467010.1029/3003JD003584.

Jarvis, P.G., McNaughton, K.G., 1986. Stomatal control of transpiration. Adv. Ecol. Res. 15, 1–49.

Kato, T., Tang, Y., Gu, S., Hirota, M., Cui, X., Du, M., Li, Y., Zhao, X., Oikawa, T., 2004a. Seasonal patterns of gross primary production and ecosystem respiration in an alpine meadow ecosystem on the Qinghai–Tibetan Plateau. J. Geophys. Res. 109 (D12109)10.1029/2003JD003951.

Kato, T., Tang, Y., Gu, S., Hirota, M., Cui, X., Du, M., Li, Y., Zhao, X., Oikawa, T., 2004b. Carbon dioxide exchange between the atmosphere and an alpine meadow ecosystem on the Qinghai–Tibetan Plateau. Chin. Agric. For. Meteorol. 124, 121–134.

Kellner, E., 2001. Surface energy fluxes and control of evapotransporation from a Swedish *Sphagnum* mire. Agric. For. Meteorol. 110, 101–123.

Li, J.L., Hong, Z.X., Luo, W.D., Li, A.G., Zhao, Y.J., 1999. A study of surface fluxes in Gerze area, Qinghai-Xizang Plateau. China J. Atom. Sci. 23 (2), 142–151.

Liu, X.D., Chen, B.D., 2000. Climatic warming on the Tibetan Plateau during recent decades. Int. J. Climatol. 20, 1729–1742.

Mahrt, L., 1998. Flux sampling strategy for aircraft and tower observations. J. Atmos. Ocean. Technol. 15, 416–429.

Monteith, J.L., Unsworth, M.H., 1990. Principles of Environmental Physics, 2nd ed. Chapman and Hall, New York, USA.

Raupach, M.R., 1998. Influences of local feedbacks on land–air exchanges of energy and carbon. Global Change Biol. 4, 477–494.

Stannard, D.I., Blanford, J.H., Kustas, W.P., Nichols, W.D., Amer, S.A., Schmugge, T.J., Weltz, M.A., 1994. Interpretation of surface flux measurements in heterogeneous terrain during the Monsoon '90 experiment. Water Resour. Res. 30, 1227–1239.

Sun, H.L., Zheng, D., 1996. Formation and Evolution of the Qinghai–Xizang Plateau.. Shanghai Science and Technology Press, Shanghai (in Chinese, with English abstract).

Webb, E.K., Pearman, G.I., Leuning, R., 1980. Correction of flux measurements for density effects due to heat and water vapor transfer. Quart. J. Roy. Meteorol. Soc. 106, 67–90.

Wilson, K., Goldstein, A., Falge, E., Aubinet, M., Baldocchi, D., Berbigier, P., Bernhofer, C., Ceulemans, R., Dolman, H., Field, C., Grelle, A., Ibrom, A., Law, B.E., Kowalski, A., Meyers, T., Moncrieff, J., Monson, R., Oechel, W., Tenhunen, J., Valentini, R., Verma, S., 2002. Energy balance closure at FLUXNET sites. Agric. For. Meteorol. 113, 223–243.

Yabuki, H., Ohata, T., Ageta, Y., 1998a. Seasonal change of land–surface processes in permafrost in permafrost region of Tibetan Plateau. 1. Moisture and heat conditions at surface–soil layer. J. Jpn. Soc. Hydrol. Water Resour. 10, 324–335 (in Japanese, with English abstract).

Yabuki, H., Ohata, T., Ageta, Y., 1998b. Seasonal change of land–surface processes in permafrost in permafrost region of Tibetan Plateau. 2. Evaporation and water budget in the surface–soil layer.. J. Jpn. Soc. Hydrol. Water Resour. 10, 336–345 (in Japanese, with English abstract).

Yao, T.D., Liu, X.D., Wang, N.L., Shi, Y.F., 2000. Amplitude of climatic changes in Qinghai–Tibetan Plateau. Chin. Sci. Bull. 45, 1236–1243.

Zheng, D., 2000. Mountain Geoecology and Sustainable Development of the Tibetan Plateau. Kluwer Academic Publishers, Dordrecht, The Netherlands.